Properties of the ZnO/PS nanocomposites obtained by sol-gel method

HONG CAI[*], HONGLIE SHEN, LINFENG LU, HAIBIN HUANG, ZHENGXIA TANG, YUGANG YIN, JIANCANG SHEN[a]

College of Materials Science & Engineering, Nanjing University of Aeronautics and Astronautics, 210016 ，Nanjing China
[a]National Laboratory of Solid State Microstructure & Department of Physics, Nanjing University, 210093, Nanjing China

In the present work we investigated the ZnO/PS nanocomposite films. The porous silicon (PS) substrates were formed by electrochemical anodization from p-type (100) silicon wafer, and the starting material for ZnO was Zinc acetate. The ZnO thin films were deposited on the PS substrate with different porosities by sol-gel spin coating technique. XRD analysis revealed that highly (002) oriented ZnO thin films were formed. The photoluminescence (PL) measurements on the ZnO/PS nanocomposite films showed three intense broadband photoluminescence emissions at around ~ 380 nm, ~ 510 nm, and ~ 750 nm. The effects of the PS substrate on the PL properties were also studied in detail.

1. Introduction

The discovery of intense photoluminescence (PL) at room temperature (RT) in the visible spectral region [1-3] from porous silicon (PS) has resulted in a great deal of research. In recent years, much effort has been focused on the elaboration of nanocomposites based on PS due to its potential applications in the silicon-based optoelectronics devices. Attempts have been made first by Canham to impregnate the pores with laser dyes [4]. Ethanolic solutions of coumarin, xanthene and oxazine dyes were used. Since then various matters have been introduced into the pores. One of the goals is to obtain white light emission devices. Generally, white light can be obtained by combining three light emitting diode (LED) chips giving red, green and blue colours [5].

ZnO is characterized by wide direct band-gap of 3.37 eV at RT and a high exciton binding energy of 60 meV. During the last few years, ZnO has been investigated as the functional materials for some electronic and optoelectronic devices, such as transparent conductive contacts, solar cells, laser diodes, ultraviolet lasers, thin films transistors [6-8], etc. Usually, PL spectra of ZnO are composed of a visible blue-green band related to a deep level defect emission and UV emission from the ZnO exciton emission [9,10]. Obviously investigations should be performed on ZnO/PS composites. Although deposition of ZnO films on PS substrates have been carried out, there are few reports concerning PL from ZnO/PS composites [5,11]. So far, different methods have been used to deposit ZnO films, such as: pulse laser deposition (PLD) [3], chemical vapor deposition (CVD) [12], RF magnetron sputtering [13], sol-gel process [14,15], etc.

In this work, ZnO films were deposited on porous silicon substrates by sol-gel spin coating technique which is simple, flexible and low cost. The structural and luminescence properties of ZnO/PS nanocomposites had been studied in detail.

2. Experimental

2.1 Preparation of substrates

The porous silicon layer was formed on p-type (100) *c*-Si wafer with the resistivity of 0.01~0.02Ω·cm using electrochemical anodization. The anodization was carried out in a mixture of HF (40 wt.%) and ethanol (AR) in 1:1 proportion. The current density is 40 mA/cm^2 and 80 mA/cm^2, respectively. After processing, the samples were cleaned by deionized water and then blown dry by Ar gas.

2.2 Deposition of ZnO thin films by sol-gel method

ZnO films were deposited on the porous silicon substrates by the spin coating sol-gel method. Zinc acetate dehydrate [Zn(CH$_3$COO)$_2$2H$_2$O], which is a precursor, was first dissolved in a 2-methoxyethanol solution along with monoethanolamine (MEA) as the sol stabilizers. After stirring for 1 h at 60 ℃, a homogeneous transparent solution with a concentration of 0.3 M zinc acetate and a 1:1 molar ration of MEA/zinc acetate dehydrate has been formed. This solution was kept for hydrolysis for 48 h at room temperature before coating. It was then spin-coated

on the above mentioned porous silicon substrates at 3000 rpm for 30 s at room temperature. To evaporate the solvent, the coatings were then dried in a furnace at 300 ℃ for 15 min in air. By repeating the coating 10 times, ZnO thin film with the thickness of ~ 120 nm was obtained. The as-deposited film was then annealed in an environment of Ar at 650 ℃ for 1 h.

In order to investigate the effects of porous silicon template on the photoluminescence properties of ZnO/PS nanocomposites, we also deposited the ZnO films on *c*-Si using sol-gel method for comparison.

2.3 Characterization

The crystallinity and orientation of the ZnO crystallites was monitored by XRD (D8 ADVANCE, Bruker) using CuK$_\alpha$ radiation having a wavelength of 1.54 Å. The microstructure of the ZnO films on PS was investigated using scanning electron microscopy (SEM; LEO-1530VP). The PL measurements were carried out using 325 nm line of He-Cd laser as an excitation light source.

3. Results and discussion

3.1. SEM

The cross-sectional SEM image of the ZnO film on PS substrate is shown in Fig. 1. It can be seen that the thickness of the ZnO thin film is ~ 120 nm. From the SEM picture, it was obvious that the ZnO thin film was closely connected with the PS substrate in a zigzag pattern and no clear clearance can be found in the interface. This may be because of the partial filling of the ZnO particles in the pores of PS. The surface of the PS layer is a sponge-like structure which consists of large number of 'pores' and 'voids'. These 'pores' and 'voids' make porous silicon an adhesive surface for accommodating ZnO into its pores. Thus, the ZnO thin film acted as a transparent capping and providing a good coverage of the crystallite surface on the PS substrate, which could improve the structural stability of the PS substrate.
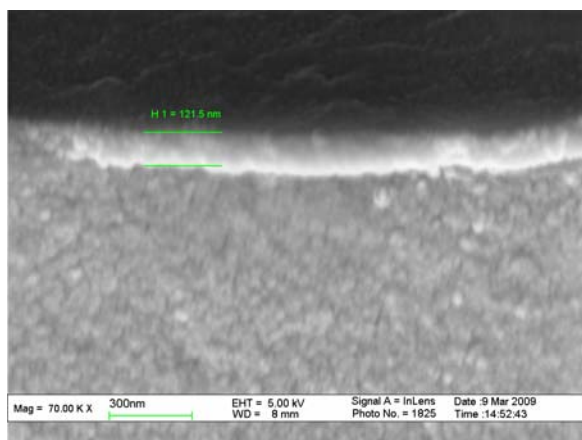
Fig. 1. SEM image of the cross-sectional ZnO/PS.

3.2. X-ray diffraction

Fig. 2 shows the XRD spectra of ZnO thin films on bare silicon (Fig. 2 (a)) and on PS substrates etched at 40mA (Fig. 2 (b)) and 80mA (Fig. 2 (c)), respectively. It is observed that all the films exhibit only (002) diffraction peak with no significant asymmetry. This indicates that all the films are polycrystalline in nature with a hexagonal wurtzite structure and c-axis oriented perpendicular to the substrate surface. The reason of c-axis-oriented growth can be explained in terms of the low surface free energies of the (002) plane. According to the previous report [16,17], the (002) face is the high-density face and is the face with the lowest free energy.
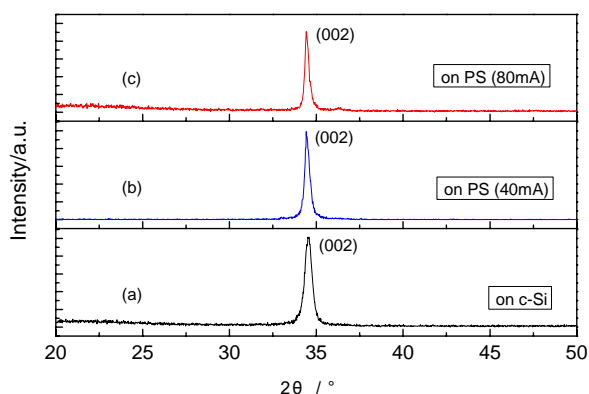
Fig. 2. XRD patterns of the ZnO films deposited on c-Si (a) and porous silicon substrates etched at (b) 40 mA, (c) 80 mA.

From Fig. 2, one can see that for all the ZnO films on PS substrates the relative intensity of the (002) diffraction peak is sharper than on the bare silicon wafer. The full-width half maximum (FWHM) value decreased from 0.49 on bare silicon wafer to 0.30 on 40mA etched PS and 0.27 on 80mA etched PS. The results implied that the special surface morphology of the PS substrate had some impact on improving the crystalline quality of the deposited ZnO thin film. In addition, the crystalline quality of the ZnO thin films increased with the increase of the etching current density, that is, the porosity of the PS substrates. The reason may be that the ZnO nano-particles that have infiltrated into the pores will establish good nucleation sites which would induce the ZnO nano-particles to grow along the preferred orientation [18]. From the XRD results, it can be seen that the porous silicon substrate can serve as a good template during ZnO growth.

When ZnO was deposited on bare silicon wafer, a rather large stress will be introduced into the ZnO thin film due to the large mismatch in the lattice constant and the thermal expansion coefficient between ZnO thin film and PS substrate [19]. From Fig. 2 (a), it can be seen that for the ZnO thin film on bare silicon wafer the (002) diffraction peak position of 2θ is at 34.52° which shifts towards higher angle compared to the value of 34.43° for

bulk ZnO. It can be attributed to the residual stress in the films [20]. According to the result of L. S. Chuah et al [21], the porous layer is a good substrate in lattice mismatch heteroepitaxy. Fig. 2 (b) and (c) reveals that for the ZnO thin films on PS substrate the (002) diffraction peak position (2θ) is at 34.42° which is very close to the corresponding value of 34.43° for bulk ZnO. The reason is that the skeleton of the porous layer is supple due to the effect of the pore structure and thus could relax the stress and limit the formation of dislocation and cracks in the ZnO thin films.

3.3 Photoluminescence studies

Fig. 3 shows the room temperature PL spectra of the ZnO/PS nanocomposites on the PS substrates etched at 40mA (Fig. 3 (a)), 80mA (Fig. 3 (b)), respectively. The PL spectrum of the PS substrate etched at 80 mA is shown in the inset of Fig. 3 and we observed a very intense emission peak at around 630 nm. The strong PL signifies the good quality of the PS substrate. From Fig. 3, it can be seen that the spectra of the ZnO/PS nanocomposite films all consist of three sharp emission peaks at about 380 nm, 510 nm and 750 nm.
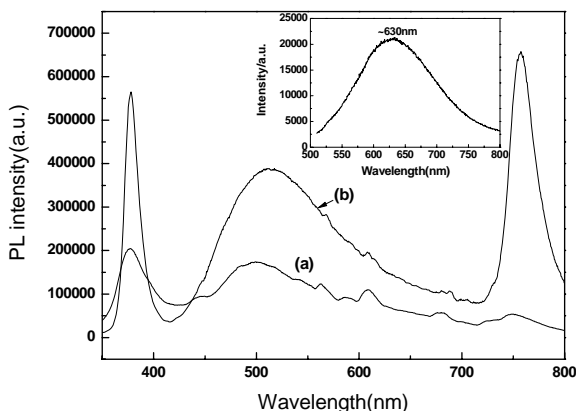
Fig. 3. Photoluminescence spectra of ZnO/PS composite films. Inset shows the PL spectra of the porous silicon.

Obviously, the ZnO/PS nanocomposite films luminesce out of the spectral range of PS emission. This indicates that the PL of the ZnO/PS nanocompsite films does not originate only from PS. The peak at around 750 nm is attributed to the PS substrate. From the inset of Fig. 3, we can see that the peak of PS substrate is at around 630 nm. This PL emission band is originated from the quantum confinement of electrons in the nanosized particle of c-Si exist in PS [22]. After ZnO coating, the red PL emission band of PS shows a red-shift from ~ 630 nm to ~ 750 nm. The reason could be that ZnO introduced into the PS surface may influence the silicon crystallite size: change in the surface structure and the interface between ZnO and porous silicon [18]. The observed intense UV emission band peak at 380 nm and green band peak at around 510 nm are apparently related to the ZnO thin films. The strong peak at 380 nm is the ultraviolet near band emission (NBE) which is due to free exciton recombination [23]. From Fig. 3, it can be found that when the current density increased from 40 mA to 80 mA, the intensity of NBE become much stronger. This phenomenon was basically in accordance with the previous XRD results: when the current density increased from 40 mA to 80 mA, the crystalline quality of the deposited ZnO thin film was improved significantly. So we think that the NBE luminescence property of the films has a close relation with the film crystallinity. The peak at ~ 510 nm is the visible emission which has been understood by an oxygen-bonding model in PS [24]. And according to the report [25], 80 mA PS would consists of more surface oxide related layer (SiO_x) than 40 mA PS. So, the enhancement of the peak at ~ 510 nm is probably originated from the increase of oxygen related luminescence centers.

4. Conclusions

We have elaborated ZnO/PS nanocomposites by the sol-gel spin coating technique which is a simple and low cost process. From various structural and optical characterizations, it has been shown that the ZnO thin films are highly (002) orientation and the ZnO/PS nanocomposites exhibits three intense broadband photoluminescence emissions at around ~ 380 nm, ~ 510 nm and ~ 750 nm. Our study revealed that the porous surface of the PS substrate play a key role to the crystalline quality and the luminescence properties of the ZnO/PS nanocomposite films. As the porosity of PS substrates increases, the crystalline quality and the PL intensity of the deposited ZnO thin film would be improved. According to the PL results of the films, the study so shows the potential applications of nanocomposites ZnO/PS films in various optoelectronic devices used in the white light region.

References

[1] L. T. Canham, Appl. Phys. Lett. **57**, 1046 (1990).
[2] M. V. Wolkin, J. Jorne, P. M. Fauchet, G. Allan, C. Delerue, Phys. Rev. Lett. **82,** 197 (1999).
[3] X. L. Wu, S. J. Xiong, D. L. Fan, Y. Gu, X. M. Bao, G. G. Siu, M. J. Stokes, Phys. Rev. B **62,** R7759 (2002).
[4] L. T. Canham, Appl. Phys. Lett. **63,** 337 (1993).

 [5] B. Zhao,Q.-S. Li, H.-X. Qi, N. Zhang, Chin. Phys. Lett. **23** 1299 (2006).

 [6] W. Z. Xu, Z. Z. Ye, Y. J. Zeng, L. P. Zhu, B. H. Zhao, L. Jiang, J. G. Lu, H. P. He, S. B. Zhang, Appl. Phys. Lett. **88**, 173506 (2006).

 [7] E. M. Wong, P. C. Searson, Appl. Phys. Lett. **74,** 2939 (1999).

 [8] R. Martins, E. Fortunato, P. Nunes, I. Ferreira, A. Marques, M. Bender, N. Katsarakis, V. Cimalla, G. Kiriakidis, Journal of Applied Physics **96**, 1398 (2004).

 [9] V. A. Fonoberow, A. A. Khan, A. A. Balandin, F. Xiu, J. Liu, Phys. Rev. B **73,** 165317 (2006).

[10] V. A. Fonoberow, A. A. Balandin, Appl. Phys. Lett. **85,** 5971 (2004).

[11] J. W. P. Hsu, D. R. Simpson, N. A. Messert, R. G. Copeland, Appl. Phys. Lett. **88,** 252103 (2006).

[12] K. Haga, P. S. Wijesena, H. Watanabe, Applied Surface Science **169**, 504 (2001).

[13] K. B. Sundaram, A. Khan, Thin Solid Films **295**, 87 (1997).

[14] S. Fujihara, C. Sasaki, T. Kimura, Applied Surface Science **180**, 341 (2001).

[15] Y. Natsume, H. Sakata, Mater, Chemical Physics **78**, 170 (2002).

[16] N. H. Tran, A. J. Hartmann, R. N. Lamb, J. Phys. Chem. B **103**, 4264 (1999).

[17] N. Fujimura, T. Nishihara, J. Xu, J. Cryst. Growth **130,** 269 (1993).

[18] R. G. Singh; Fouran Singh; V. Agarwal; R. M. Mehra, Journal of Physics D-Applied Physics **40**, 3090 (2007).

[19] H.-C. Hsu, C.-S. Cheng, C.-C. Chang, S. Yang, C.-S. Chang, W.-F. Hsieh, Nanotechnology **16,** 297 (2005).

[20] M. Chen, Z.L. Pei, C. Sun, L.S. Wen, X. Wang, J. Cryst. Growth **220,** 254 (2000).

[21] L. S. Chuah, Z. Hassan, H. A. Hassan, J. Alloys and Compounds, doi: 10.1016/j.jallcom. 2009. 01. 085, (2008).

[22] C. H. Chen, Y. F. Chen, Appl. Phys. Lett. **75,** 2560 (1999).

[23] D. M. Bagnall, Y. F. Chen, Z. Zhu, T. Yao, M. Y. Shen, T. Goto, Appl. Phys. Lett, **73,** 1038 (1998).

[24] J. Chen, T. Fujika, Japan. J. Appl. Phys. 42, 602 (2003).

[25] R. Prabakaran et al., J. Non-Cryst. Solids, doi:10.1016/j.jnoncrysol.2007.09.105, 2008.

[*]Corresponding author: yueliang@nuaa.edu.cn